JOURNAL OF GEOPHYSICAL RESEARCH, VOL. 113, D12118, doi:10.1029/2007JD009424, 2008

Seasonal forecast for local precipitation over northern Taiwan using statistical downscaling

Jung-Lien Chu,[1] Hongwen Kang,[2] Chi-Yung Tam,[2] Chung-Kyu Park,[2,3] and Cheng-Ta Chen[1]

Received 17 September 2007; revised 8 January 2008; accepted 28 February 2008; published 28 June 2008.

[1] This study investigates the potential of predicting local precipitation over northern Taiwan using statistical downscaling of large-scale circulation variables from global climate models (GCMs). Historical hindcast data of 500 hPa geopotential height (Z500) and sea level pressure (SLP) from six different GCMs, with the target season of being that of June, July, and August (JJA), are used as predictors for downscaling. Singular value decomposition analysis (SVDA) using observational data reveals that the rainfall over northern Taiwan is strongly coupled with a prominent tripole pattern of Z500 (SLP) field over the western North Pacific/East Asian coast. SVDA using model SLP or height field and station rainfall as input also gives similar results, indicating that most models can capture this mode of covariability. SLP and Z500 from models are then used for local rainfall prediction based on their relationship, which is drawn from the SVDA. For every station considered in this study, downscaled prediction shows considerable improvement when compared with model output. In particular, downscaling is able to correct the erroneous sign of model rainfall prediction. However, a few models show very low skill in their downscaled precipitation. For these models, the correlation between observed rainfall and simulated Z500 (SLP) leading SVD patterns is found to be weak. The performance based on the average of downscaled prediction using Z500 and SLP is also evaluated. In general, the average prediction is more stable and skillful when compared with results based on one predictor. Overall, this study demonstrates that useful regional climate information can be obtained from downscaling using large-scale variables from coarse-resolution GCM products.

Citation: Chu, J.-L., H. Kang, C.-Y. Tam, C.-K. Park, and C.-T. Chen (2008), Seasonal forecast for local precipitation over northern Taiwan using statistical downscaling, *J. Geophys. Res.*, *113*, D12118, doi:10.1029/2007JD009424.

1. Introduction

[2] The East Asian Summer Monsoon (EASM) region is noted for its complex space-time rainfall variability. The complexity of the monsoon system makes it hard to have skillful predictions in the EASM region. General circulation models (GCMs) have become the main tool for seasonal prediction. Though large-scale features of atmospheric variability in the tropics can be reasonably captured [see, e.g., *Lau*, 1985; *Rowell*, 1998], GCMs still have considerable difficulties in faithfully simulating regional climate correlations [*Grotch and MacCracken*, 1991; *Xu*, 1999]. Owing to their relatively coarse resolution, land-sea contrast and topography in the regional scale cannot be properly represented in global models. The difficulty in skillfully predicting the EASM broad-scale climate using GCMs makes regional climate forecast an even more challenging problem [*Sperber and Palmer*, 1996; *Wang et al.*, 1998; *Sperber et al.*, 2001; *Kang et al.*, 2002].

[3] Various methods of downscaling have been developed in order to overcome the inadequacies of GCMs in simulating local climate conditions. They can be categorized into two types. One is the method of dynamical downscaling. High-resolution simulation is obtained using a regional climate model, which in turn is driven by the outputs of a coarser resolution GCM. This method has the potential of simulating extreme events [*Díez et al.*, 2005]. However, high-resolution simulations can be computationally expensive, and a lot of storage space is required for archiving model outputs. The other type is statistical downscaling [*Von Storch et al.*, 1993]. The goal is to discover a stable relation between GCM outputs and a variable of the local climate. This relationship is exploited in order to predict elements of the regional climate using GCM products. Statistical downscaling has come to be widely used because of its lesser computational requirement.

[4] Most statistical downscaling schemes are based on regression or similar methods [*Giorgi et al.*, 2001; *Benestad*, 2004]. *Wetterhall et al.* [2005] used sea level

[1]Department of Earth Sciences, National Taiwan Normal University, Taipei, Taiwan.
[2]Science Division, APEC Climate Center (APCC), Busan, South Korea.
[3]Climate Prediction Division, Korea Meteorological Administration, Seoul, South Korea.

0148-0227/08/2007JD009424$09.00

Table 1. Description of Hindcast Experiments Used in This Study

Acronyms	Institution	Model Resolution	Data Type
CWB	Central Weather Bureau (Chinese Taipei)	T42 L18	SMIP/HFP
HMC	Hydrometeorological Centre of Russia (Russia)	1.12° × 1.4° L28	SMIP/HFP
JMA	Japan Meteorological Agency (Japan)	T63 L40	SMIP/HFP
METRI	Meteorological Research Institute (South Korea)	4° × 5° L17	SMIP/HFP
MGO	Main Geophysical Observatory (Russia)	T42 L14	SMIP/HFP
NCEP	National Centers for Environmental Prediction (a coupled forecast system) (U.S.A.)	T62 L64	CMIP/HFP

pressure (SLP) as a predictor and found increased skill in predicting the seasonal mean precipitation using analogue-based downscaling. *Feddersen and Andersen* [2005] also reports skillful predictions of temperature and precipitation by statistical downscaling.

[5] The focus of this study is the application of statistical downscaling for regional climate prediction over Taiwan. In particular, a downscaling scheme for predicting summer precipitation over northern Taiwan will be developed. The results of downscaling based on various GCM hindcast experiment data sets will be analyzed. The outline of this study runs as follows. Section 2 introduces the model data used and the method of downscaling. Analyses and results of downscaling are described in section 3. A summary and some discussions are presented in section 4.

2. Data and Methodology

2.1. Model Experiments and Station Data

[6] In the present study, data from hindcast experiments from six different global models with the target season of June, July, and August (JJA) are used for statistical downscaling. These data sets are taken from the SMIP-type historical forecasts with 1-month lead time, for the period of 1983–2003, SMIP being short for the Seasonal Prediction Model Intercomparison Project [*Kang et al.*, 2004]. They were run by six operational centers, and are archived at the Asia-Pacific Economic Cooperation Climate Center (APCC). For the hindcast experiments run by the Central Weather Bureau (CWB) [*Liou et al.*, 1997], the Hydrometeorological Centre of Russia (HMC) [*Tolstykh*, 2003] and the Main Geophysical Observatory (MGO) [*Shneerov et al.*, 1999], the Sea Surface Temperature (SST) used in seasonal prediction is based on observed persistent SST anomalies. For the Japan Meteorological Agency (JMA) [*Kanamitsu et al.*, 1983] and the Meteorological Research Institute (METRI) [*Baek et al.*, 2002], predicted SST information is used. The National Centers for Environmental Prediction (NCEP) [*Saha et al.*, 2006] forecasting system is a fully coupled model. It is noteworthy that the driving boundary SSTA forcings used in these different models are not the same. Therefore it is expected that part of differences among model simulations is due to the use of different forcings. The assumption of persistent SST anomalies in model hindcast exercise should in general lead to larger model bias when the forecast lead time increases. Almost all the ENSO forecast models (both statistical and dynamical) produce better prediction skill for tropical pacific SSTA than simple persistent SSTA when the lead time is more than one month [*Barnston et al.*, 1999]. Compared with the two-tier forecast systems (with either persistent or predicted SSTA), systematic model bias in SST simulation cannot be removed from the coupled forecast system of NCEP. However, the one-tier coupled forecast allows local air-sea interactions; it is not the case with the two-tier system, which is typically run with SST as the boundary forcing. It has been shown that the coupled atmospheric and oceanic processes are very important in simulating the realistic SST-rainfall relationship for the Asian-Pacific summer monsoon region [*Wang et al.*, 2005]. For a model driven by persistent SST anomalies, the anomalies do not change with time during the integration, but climatologic SST fields change monthly. For a 2-tier forecast model forced by predicted SST anomalies, monthly anomalies are used as part of boundary condition with linear interpolation through time. Although the SST anomalies are not identical in the different models that are used to construct the multimodel ensemble, the individual model forecast system and strategies remain consistent during all the hindcasts. Therefore the statistical downscaling method developed here should still be applicable to the possible future forecasts. Table 1 provides a summary of data sources and model experiments. All hindcast data are interpolated on a 2.5° × 2.5° grid for analyses.

[7] During the season of summer, northern Taiwan is in the lee side of The Central Mountains, which extends from the north of Taiwan to the south. Abundant moisture carried by prevalent southwesterly wind is baffled by The Central Mountains from arriving northern Taiwan. Although the Meiyu front brings a lot of precipitation to northern Taiwan in the early summer, northern Taiwan is relatively dry in this period. On the other hand, the tripole pattern of large-scale circulation during the East Asian summer also affects the rainfall in northern Taiwan [*Hsu and Lin*, 2007]. In the positive phase of the tripole pattern, the southwestward shift of the Pacific subtropical anticyclone corresponds to a below-normal rainfall in northern Taiwan, which would make northern Taiwan drier. Thus in order to prevent drought, the management of water resources and the local rainfall forecasting have become an important topic for northern Taiwan. Station data of precipitation over Taiwan for the period of 1950–2006 are provided by the CWB. In this study, six of these stations in northern Taiwan are studied. Their locations are shown in Figure 1. In addition, NCEP-NCAR Reanalysis fields are also used as observational data in this study.

2.2. Choice of Predictors

[8] Statistical downscaling makes use of long-term GCM hindcast data to derive robust relationships between observations and model outputs. The information is then used for choosing suitable meteorological variables as predictors.

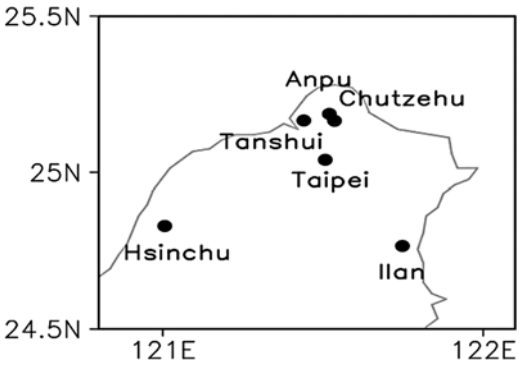

Figure 1. Location of the six stations in northern Taiwan considered in this study.

Two conditions should be satisfied in selecting the right variable. One is that it has to be well simulated by the GCM [*Wilby et al.*, 1999]. The other is that there should be a stable relation between the predictor and the predictand. For instance, the variable with the highest correlation coefficient with the predictand can be a good choice for a predictor [*Kang et al.*, 2007]. Commonly used large-scale variables for predicting precipitation include the geopotential height [*Von Storch and Zwiers*, 1999], SLP [*Wetterhall et al.*, 2005], geostrophic wind [*Wilby et al.*, 1998] and wind speed [*Murphy*, 1999].

[9] In addition to selecting predictors, it is also important to determine the domain over which predictor values are considered. The place where the correlation coefficient between a predictand and a predictor is zero can be considered to be the boundary of a domain [*Benestad*, 2004]. Another basis for the selection of a domain is that it should be large enough to resolve the relevant large-scale pattern and encompass corresponding observations [*Feddersen and Andersen*, 2005].

[10] Based on the results of correlation analyses between various large-scale variables and the station rainfall of interest, 500 hPa geopotential height (Z500) and SLP are used as predictors and the domain of analysis is chosen to be 80°–160°E and 0°–60°N.

2.3. Statistical Downscaling Method

[11] In this study, a combination of EOF truncation and SVDA is used to obtain stable statistical relationships between large-scale circulation and regional precipitation. Before downscaling is applied, the time series of large-scale variables are reconstructed using their respective EOFs and principal components as a means of noise filtering. Here, the first ten leading modes for the large-scale variables are retained. SVDA is then used to extract coupled patterns between large-scale circulation and regional precipitation. In SVDA, the coupled patterns mentioned above can be expressed in the equation, which is as follows:

$$Z_{predictor}(t,x) = \sum_{i=1}^{m} U_i(x)S_i(t)$$

$$Z_{predic\ tan\ d}(t,x) = \sum_{i=1}^{m} R_i(x)K_i(t)$$

Here, m is the total number of SVD modes. The large-scale circulation anomaly field and the observed station rainfall anomaly fields, $Z_{predictor}$ (t, x) and $Z_{predic\ tan\ d}$ (t, x), are normalized to have mean zero and standard deviation one. $U_i(x)$ and $R_i(x)$ indicate the singular vector of the predictor and of the predictand respectively in ith mode. $S_i(t)$ and $K_i(t)$ denote respectively the time expansion coefficient of the ith SVD mode for large-scale predictor and predictand.

[12] Then the following downscaling transfer function will be used.

$$PR_j(t,x) = \sum_{i=1}^{n} S_i(t)R_i(x)$$

Here $PR_j(t, x)$ indicates the downscaled prediction, and n is the total number of SVD modes retained. In this study, the leading six modes are retained. Cross-validation was carried out to evaluate the skill of the downscaling scheme. In the cross-validation, 1-year rainfall data are excluded from the data set and the rainfall data of the other years are defined into the training period. Then a prediction based on the training period is made for the excluded year [*Michaelsen*, 1987]. The corresponding climatology and anomaly fields for both predictor and predictand are also redefined at the same time, and that will prevent the signal of forecast year from being included in the training period. This procedure is repeated for 21 times, thus yielding rainfall predictions for 21 years for validation. The detail of the method of downscaling can be found by *Kim et al.* [2004], *Feddersen et al.* [1999], *Feddersen and Andersen* [2005], and *Kang et al.* [2004]. The same process is repeated for the hindcast data set of each of the six models. We also consider the results of downscaling obtained by averaging the six downscaled outputs from all models.

3. Results

3.1. Relationship Between Regional Rainfall and Observed Large-Scale Circulation

[13] For the purpose of obtaining a first glimpse of the interannual variability of rainfall over northern Taiwan, an EOF analysis for JJA precipitation is carried out. The leading EOF pattern is given in Figure 2. This EOF mode accounts for 86% of the total variance, and is characterized by the same sign of rainfall anomalies at each station. As will be shown subsequently, this dominant mode is closely tied to the circulation over the EASM region.

[14] SVD analysis is now used to unveil any robust modes of covariability between large-scale variables and station rainfall. Figure 3 gives spatial patterns for the first SVD mode using station precipitation and Z500 as input data, and those using precipitation and SLP. For the Z500 field, a tripole can be discerned in the East Asian region, which is characterized by a wave-like pattern with centers of action along the East Asian coast. There is a positive center over Taiwan, a negative center over Japan and the Korea peninsula, and a positive anomaly is found over the Sea of Okhotsk. The corresponding rainfall pattern shows suppressed precipitation for all stations over northern Taiwan, similar to the 1st EOF of rainfall (see Figure 2). A similar pair of patterns is found for the leading SVD mode for precipitation and SLP, with an obvious north-south oriented

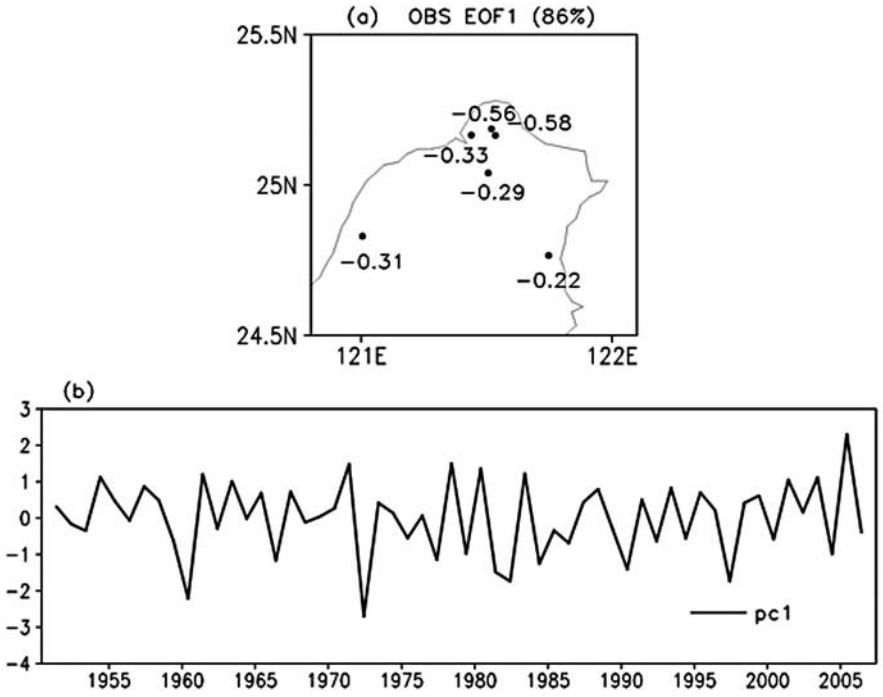

Figure 2. (a) Spatial pattern of the first EOF for station precipitation in northern Taiwan during JJA, for the period of 1951–2006. (b) The principal component of the leading EOF.

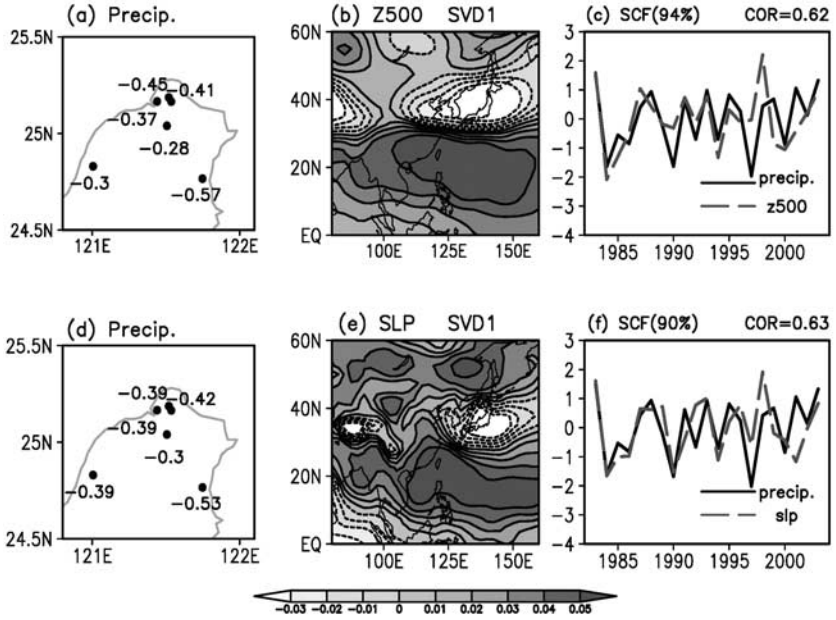

Figure 3. Leading SVD mode spatial patterns of (a) the observed station precipitation in northern Taiwan and (b) the observed Z500 in East Asia during JJA. (c) Normalized expansion coefficients corresponding to precipitation and Z500. The leading SVD spatial patterns of (d) the observed station precipitation and (e) the observed SLP in East Asia during JJA. (f) Normalized expansion coefficients for precipitation and SLP (Dotted contours represent negative values in Figures 3b and 3e. Data for the period of 1983–2003 are used.

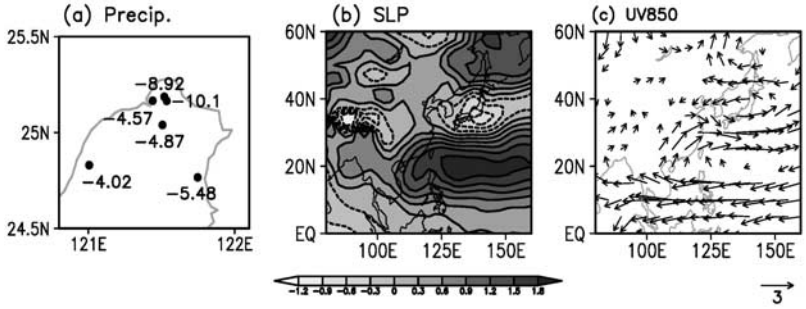

Figure 4. Dry-minus-wet composites of (a) station precipitation (unit: mm/d), (b) observed SLP field (contours in interval of 0.3mb), and (c) observed 850 hPa wind field (unit for scale arrow: 3m/s) during JJA. (wet years: 1984, 1986, 1990, 1997, and 2000; dry years: 1988, 1993, 1995, and 2003).

tripole corresponding to the latter precipitation field. The time series of expansion coefficients corresponding to the leading SVD mode for precipitation and Z500, and for SLP, are given in Figure 3c and 3f, respectively. The moderately high correlation between the expansion coefficients suggests that the rainfall and Z500 (or SLP) are coupled on interannual timescale. Overall, the results indicate that suppressed precipitation over northern Taiwan is associated with a large-scale tripole pattern in the SLP or Z500 field, with positive centers of action over Taiwan and also over the Sea of Okhotsk to northeastern Eurasia, and a negative center over Japan. In addition, the Squared Covariance Fraction (SCF) between Z500 (or SLP) and station precipitation for the first SVD mode is about 90%. These results provide a basis for choosing Z500 and SLP in predicting station rainfall over northern Taiwan during JJA.

[15] To further elucidate the relationship between the large-scale circulation and station rainfall corresponding to this SVD mode, we designed composite maps of rainfall, for SLP and 850 hPa wind. On the basis of the SVD expansion coefficients, the years of 1984, 1986, 1990, 1997, and 2000 are selected as wet years, whereas 1988, 1993, 1995, and 2003 are selected as dry years. A dry-minus-wet composite map is shown in Figure 4. It can be seen that, when dry condition prevails, there is an anomalous anticyclone over a broad region in the western Pacific, covering Taiwan. A tripole pattern can be clearly seen in the SLP composite, with consistent low-level circulation anomalies. Note that the anomalous wind field is strikingly similar to that associated with the positive phase of the dominant rainfall pattern in the EASM region studied by *Hsu and Lin* [2007].

3.2. Relationship With Model Variables

[16] The relationship between station precipitation and large-scale circulation features in models is now presented. Figures 5 and 6 show the spatial patterns of station precipitation and circulation variables associated with their leading SVD modes for each model. It is encouraging that the model Z500 features are consistent with those to be obtained from observation (see Figure 5). In particular, there is a broad-scale positive anomaly in the western Pacific, covering Taiwan, and a negative signal is found near Japan. Accompanying these is reduced rainfall over the northern part of Taiwan, which is in agreement with observation. However, details of the Z500 pattern vary from one model to another. For example, the positive signal north of Japan (see Figure 3b) is absent in HMC and NCEP models, while it is shifted westward for JMA. The negative center over Japan and the Korea peninsula found in observation is located too far north in the METRI counterpart. When compared with the observational result (see Figure 3c), the correlation between expansion coefficients of station precipitation and Z500 is relatively low for JMA, METRI, and NCEP data. For CWB, HMC, and MGO, the correlation coefficient is comparable to the case in observation ($\sim$0.6).

[17] Figure 6 gives the first SVD mode using SLP and station precipitation from each model as input. In broad agreement with observation, most model SLP patterns show a positive anomaly over the western Pacific, and a negative anomaly at 30°–40°N. However, details of the tripole feature of the observed anomalies SLP are not well captured in every model. For instance, a northward shift or expansion of the negative anomaly is found in HMC and NCEP. The negative center of action near Japan is weakened or even absent for CWB and JMA. For the correlation between expansion coefficients of precipitation and SLP, those from JMA, METRI, MGO, and NCEP are relatively low, while those from CWB and HMC are comparable to the observational value.

[18] In summary, the spatial patterns for the leading SVD modes between large-scale variables (Z500 and SLP) and station precipitation for most models resemble their respective observational counterpart. It can be found from the model hindcast data sets that there is a prominent pattern of anomalous high over western Pacific and anomalous low over Japan associated with suppressed rainfall in northern Taiwan. However, a number of models seem to have difficulty in capturing the high pressure center over the Sea of Okhotsk. It is also noteworthy that the correlation between the expansion coefficients for the rainfall and Z500 (SLP) fields is especially low for some models runs ($\sim$0.36 compared with $\sim$0.6 in observations). In other words, the large-scale circulation features in these GCMs seem to be loosely coupled with station rainfall variability. As will be seen in the next section, this weak coupling might lead to a low skill in the downscaled rainfall prediction based on these models.

3.3. Downscaling Prediction of Station Rainfall

[19] We now compare the results of precipitation predictions based on raw model outputs and those from down-

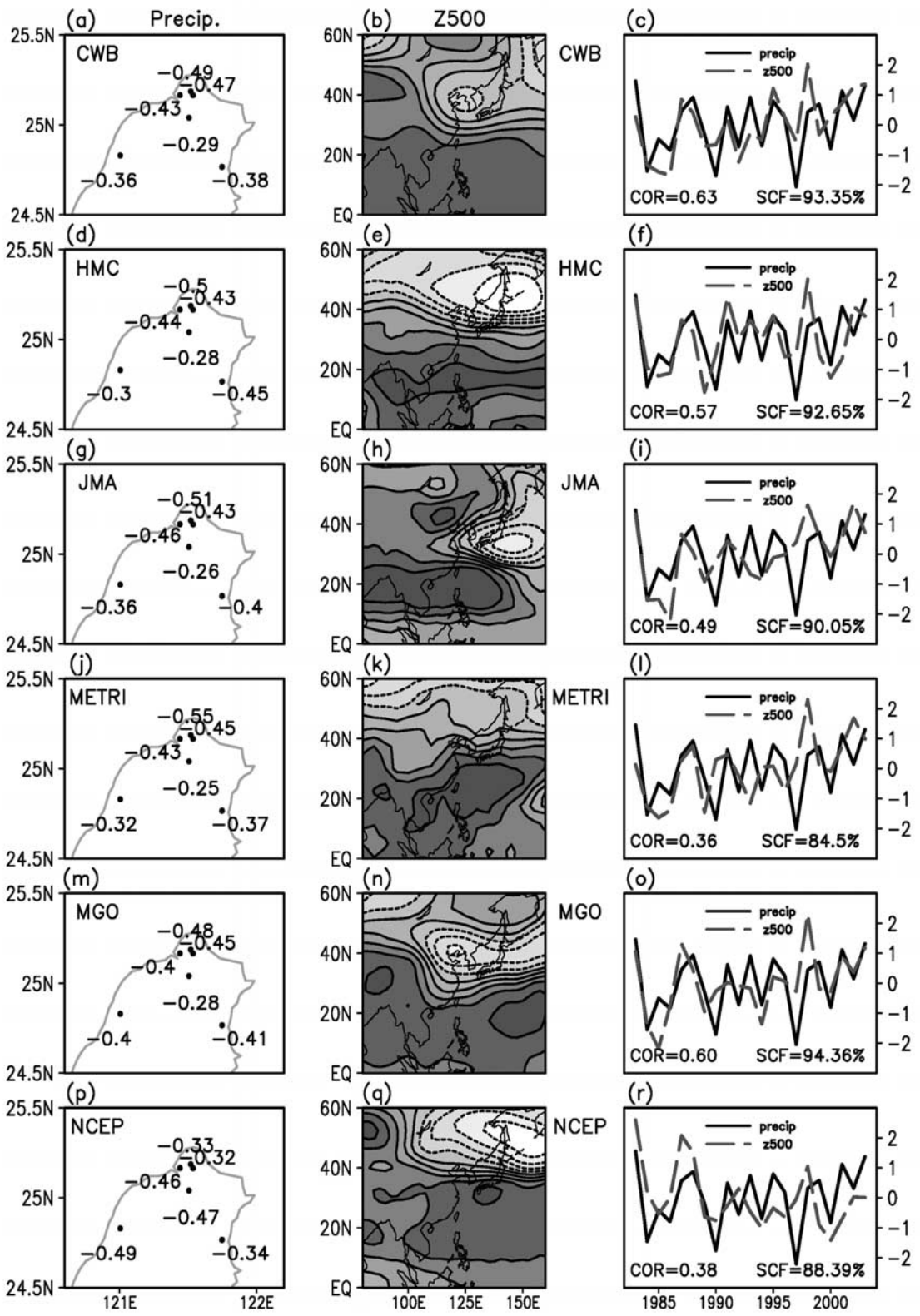

Figure 5. Leading SVD patterns of (a), (d), (g), (j), (m), (p) the observed station precipitation in northern Taiwan, (b), (e), (h), (k), (n), (q) model Z500, and (c), (f), (i), (l), (o), (r) expansion coefficients for precipitation and Z500 based on CWB (Figures 5a and 5b), HMC (Figures 5d and 5e), JMA (Figures 5g and 5h), METRI (Figures 5j and 5k), MGO (Figures 5m and 5n), NCEP (Figures 5p and 5q) hindcast data during JJA for the period of 1983–2003.

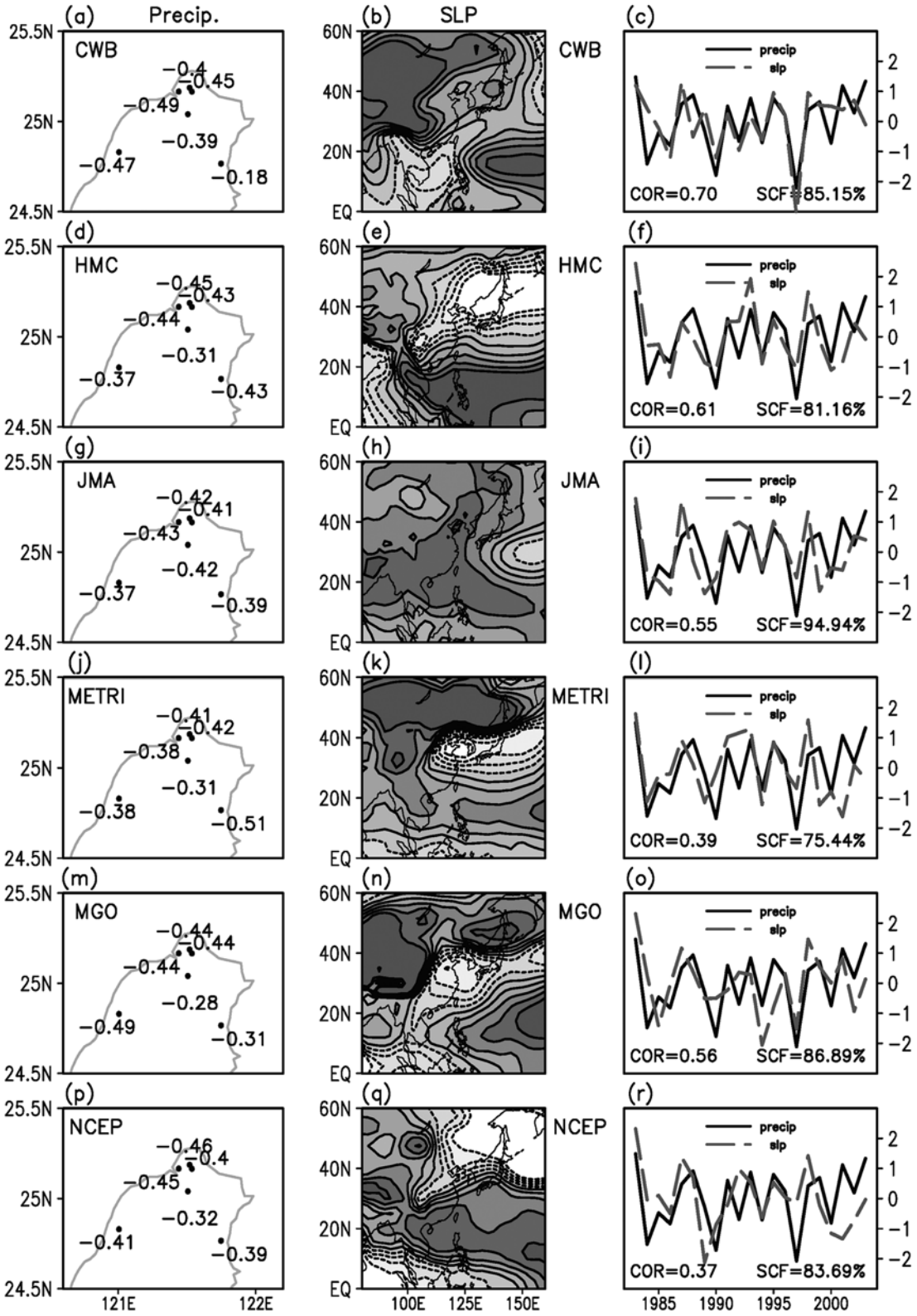

Figure 6. Same as Figure 5, but for station precipitation and model SLP.

scaling. Figure 7 shows the temporal correlation between model simulated precipitation and observational records for each station location during JJA. Models' rainfall is calculated by averaging the rainfall data of the surrounding nine gird points for each station location. It can be seen that most models show no skill in predicting station rainfall. The correlation between the rainfall averaged over all stations in northern Taiwan and that from simulation is negative for

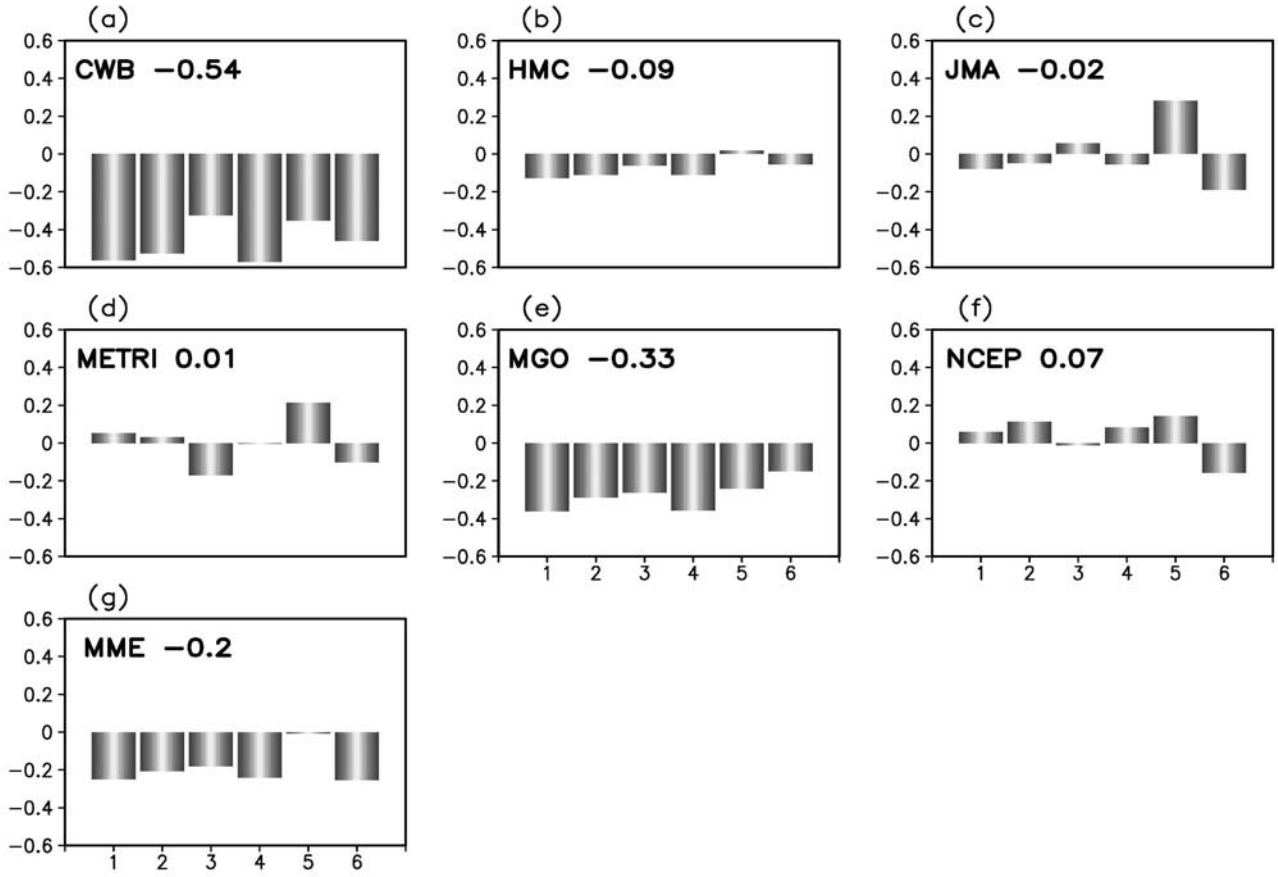

Figure 7. Correlation coefficients between the observed JJA station precipitation and precipitation from (a) CWB, (b) HMC, (c) JMA, (d) METRI, (e) MGO, (f) NCEP model, and (g) MME average of model output. Numbers on the horizontal axes represent stations located at Tanshui, Anpu, Taipei, Chutzehu, Ilan and Hsinchu. Correlation coefficients between the average precipitation for all stations and the corresponding mean precipitation from models are given at the top left of each panel.

every model. After the Multi-Model Ensemble (MME) mean (i.e., simple average of outputs from all models) is taken, the correlation coefficient for the averaged precipitation of the six stations is −0.2.

[20] On the other hand, downscaled products using model output show considerably the skill in predicting station-scale precipitation. Figure 8 gives the correlation between observed rainfall and downscaling prediction using Z500 as a predictor. There is evidence of great improvement of prediction skill. The correlation is positive between northern Taiwan averaged precipitation and the downscaled output for every model. In particular, predictions based on CWB, HMC and JMA give positive correlation coefficients for every station. As for the MME mean of downscaled outputs, the six-station averaged value of correlation coefficients is 0.49.

[21] When we compare Figure 5 with Figure 8, it can be seen that hindcasts from CWB, HMC and MGO give the highest correlation between expansion coefficients of rainfall and model Z500 patterns for their leading SVD modes. The downscaled predictions from these three models also show the highest value of correlation coefficients. Thus there is a strong association between station rainfall and the model Z500 field. Such a strong relationship, which is similar to that found in observation, leads to a good prediction of local precipitation using model large-scale variables.

[22] The correlation coefficients for downscaled outputs using SLP as a predictor are given in Figure 9. High correlation coefficients are found for downscaled precipitation from CWB, HMC, and JMA hindcasts, and also for that based on MME average. Again, there is relatively high correlation between SVD expansion coefficients for precipitation and SLP for those models with skillful downscaling prediction. The only exception seems to be MGO hindcasts when SLP is used as a predictor. While the temporal correlation is high between the expansion coefficients of SLP and rainfall, downscaling using MGO outputs is not particularly skillful. One possible reason for this could be found upon closer inspection of the SLP pattern corresponding to the first SVD mode (see Figure 6). It shows a negative SLP anomaly over Taiwan, which is opposed to the positive center over the same region in observation (see Figure 3). The erroneous circulation in the leading mode of SLP thus captured could deteriorate the skill of downscaled prediction from this model.

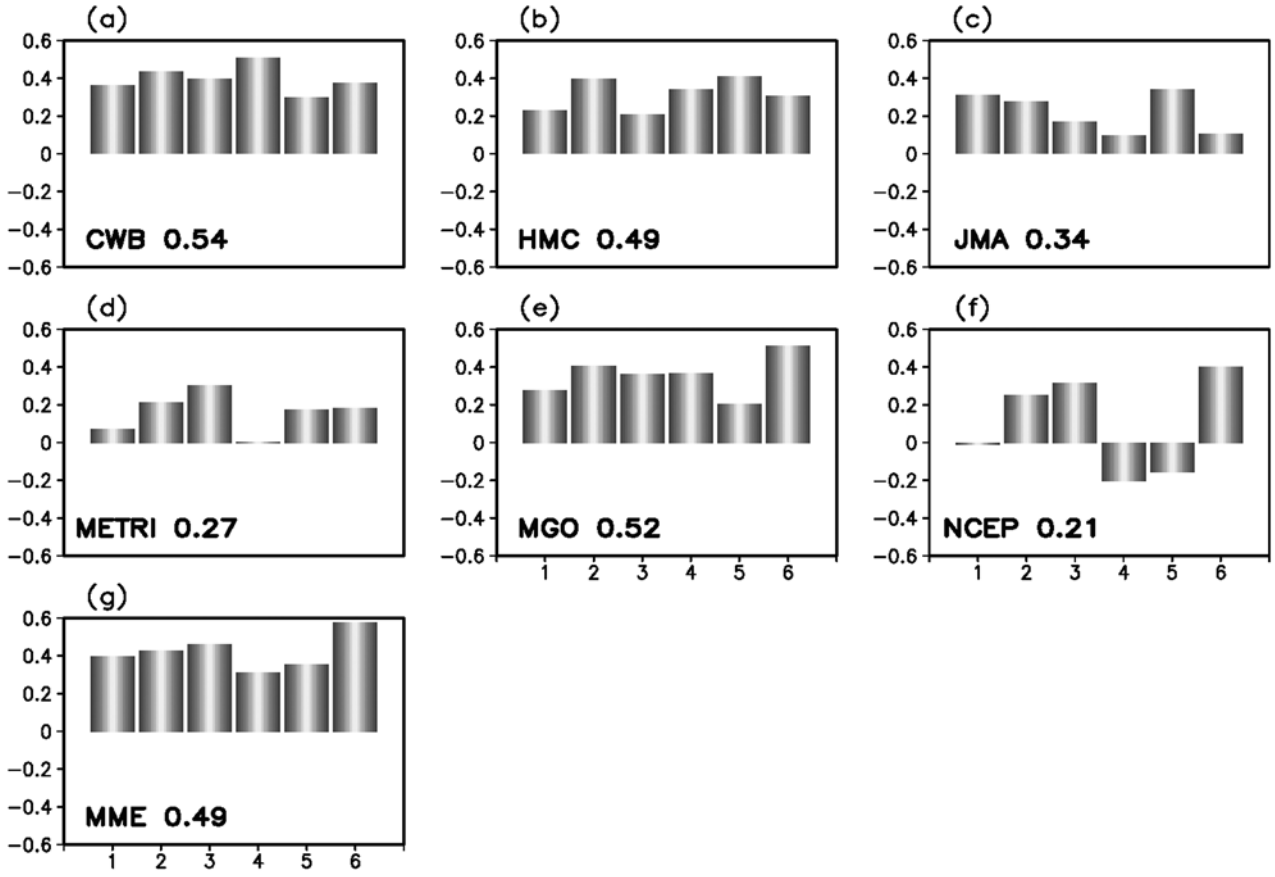

Figure 8. Same as Figure 7, but for the downscaling result using model Z500 output as a predictor.

[23] After examining the skill of downscaling based on each predictor, the results using two predictors are shown in Figure 10. For each model, downscaling is carried out by using Z500 and SLP separately, and the final prediction is the simple average of the two downscaled products. Compared with prediction based on a single predictor (see Figures 8 and 9), the prediction based on the downscaled output involving two predictors gives a better performance for the area-averaged precipitation. Although the anomaly correlations are not the standard verification system for long-range forecasts suggested by WMO, there are a considerable number of studies for forecast system evaluation that still use anomaly correlation to assess the forecast skill. In general, the standard tercile skill score such as Gerrity skill score is in good agreement with anomaly correlation [*Murphy*, 1988].

[24] Finally, we compare the observed precipitation to predictions based on various methods, on a year-to-year basis. Figure 11 shows the observation, MME average of raw model output, downscaled prediction using Z500, SLP, and Z500 and SLP together. Note that the raw MME output has been rescaled by the ratio of the standard deviation of the observed precipitation to that from simulations. It is immediately obvious that the model rainfall and the observational record tend to have the opposite sign. On the other hand, downscaling can correct the sign of rainfall prediction. For example, during 1983–1987, 1989, 1990, 1997, 1998, and 2002, downscaled results give the same sign as the observed station precipitation, while the model output and observation are out of phase. For the year of 1998, downscaling successfully predicts the sign of rainfall anomaly, but its amplitude is too strong when compared with that found in station data. It is possible that the model response is overestimated in this strong La Nina year. The method of downscaling successfully corrects the sign of prediction but fails to correct its amplitude. Results from Figure 11 also suggest that downscaling based on Z500 and SLP together gives a stable and skillful prediction. Overall, our study demonstrates that downscaled precipitation based on large-scale variables from GCMs is useful in regional climate prediction, which corroborates coarse-resolution forecast products from global climate models.

[25] In observed SLP field, the large-scale tripole pattern plays an important role for the rainfall over northern Taiwan. The southwestward shift of the Pacific subtropical anticyclone, that is, the positive phase of the tripole pattern defined by *Hsu and Lin* [2007], prohibits moisture that comes from the South China Sea and the western North Pacific warm pool from transferring to Taiwan. Although the tripole pattern cannot be well simulated by several models, the prediction skill for northern Taiwan rainfall is still improved after downscaling. One possible reason may be that, from the statistic point of view, a long-term stable relation between the simulated large-scale circulation and

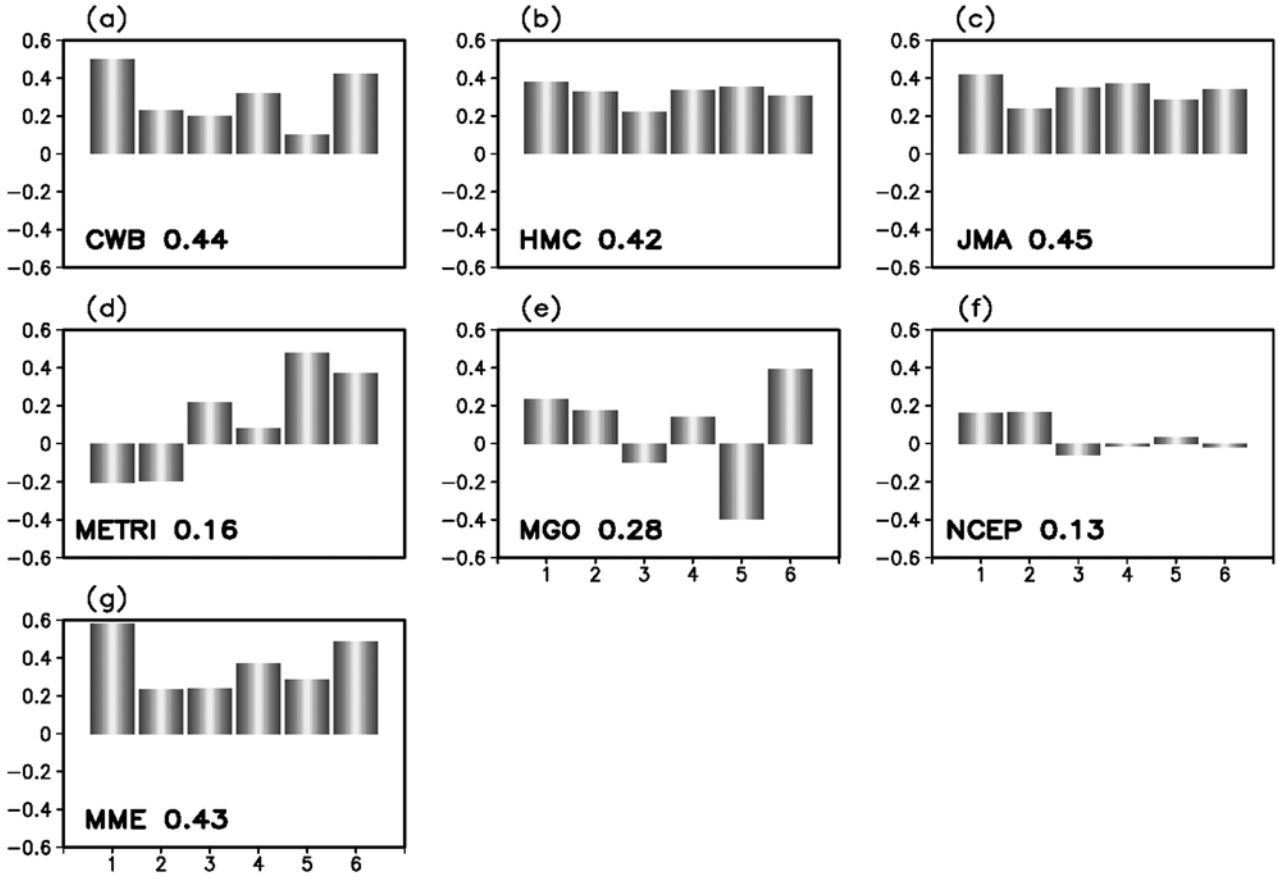

Figure 9. Same as Figure 7, but for the downscaling result using model SLP output as a predictor.

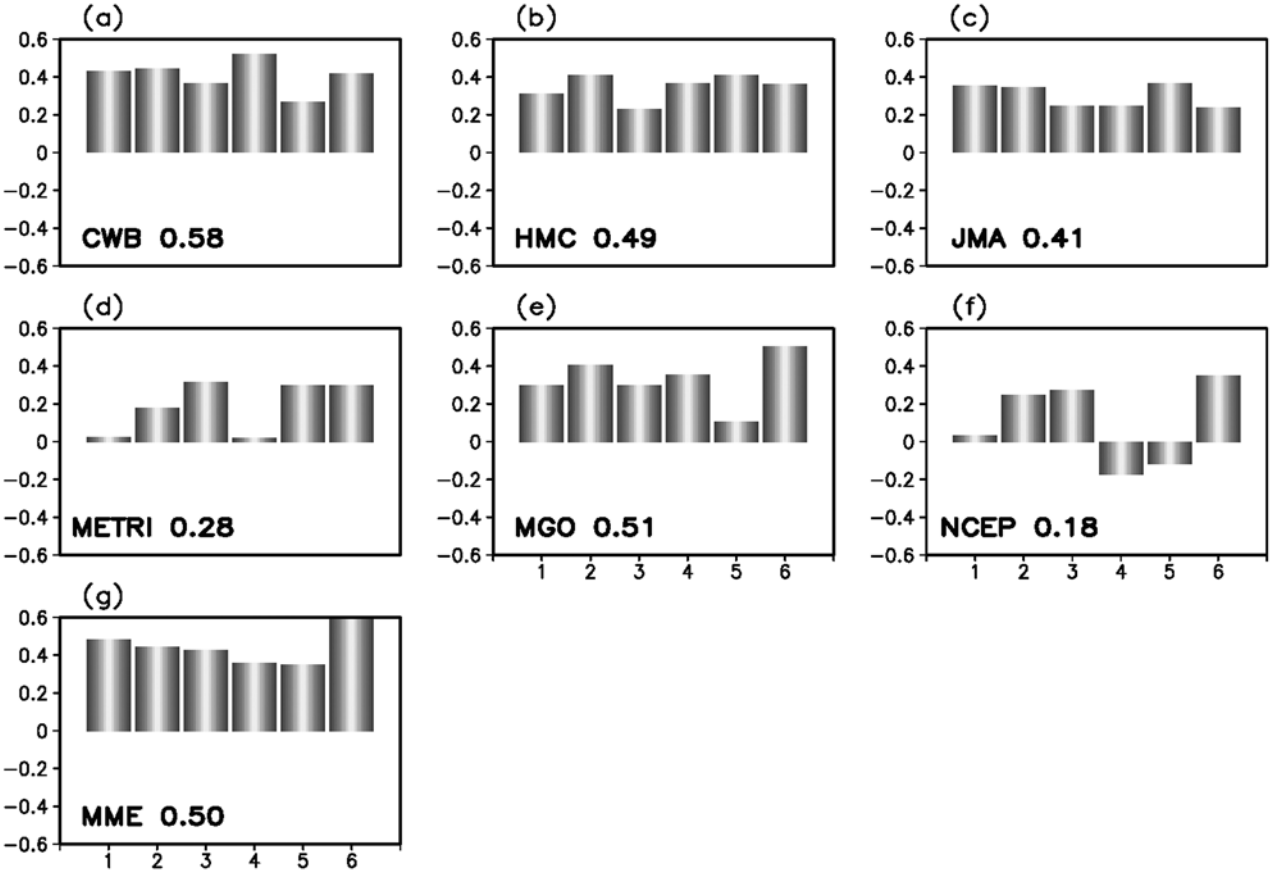

Figure 10. Same as Figure 7, but for the downscaling result using model SLP and Z500 output as predictors.

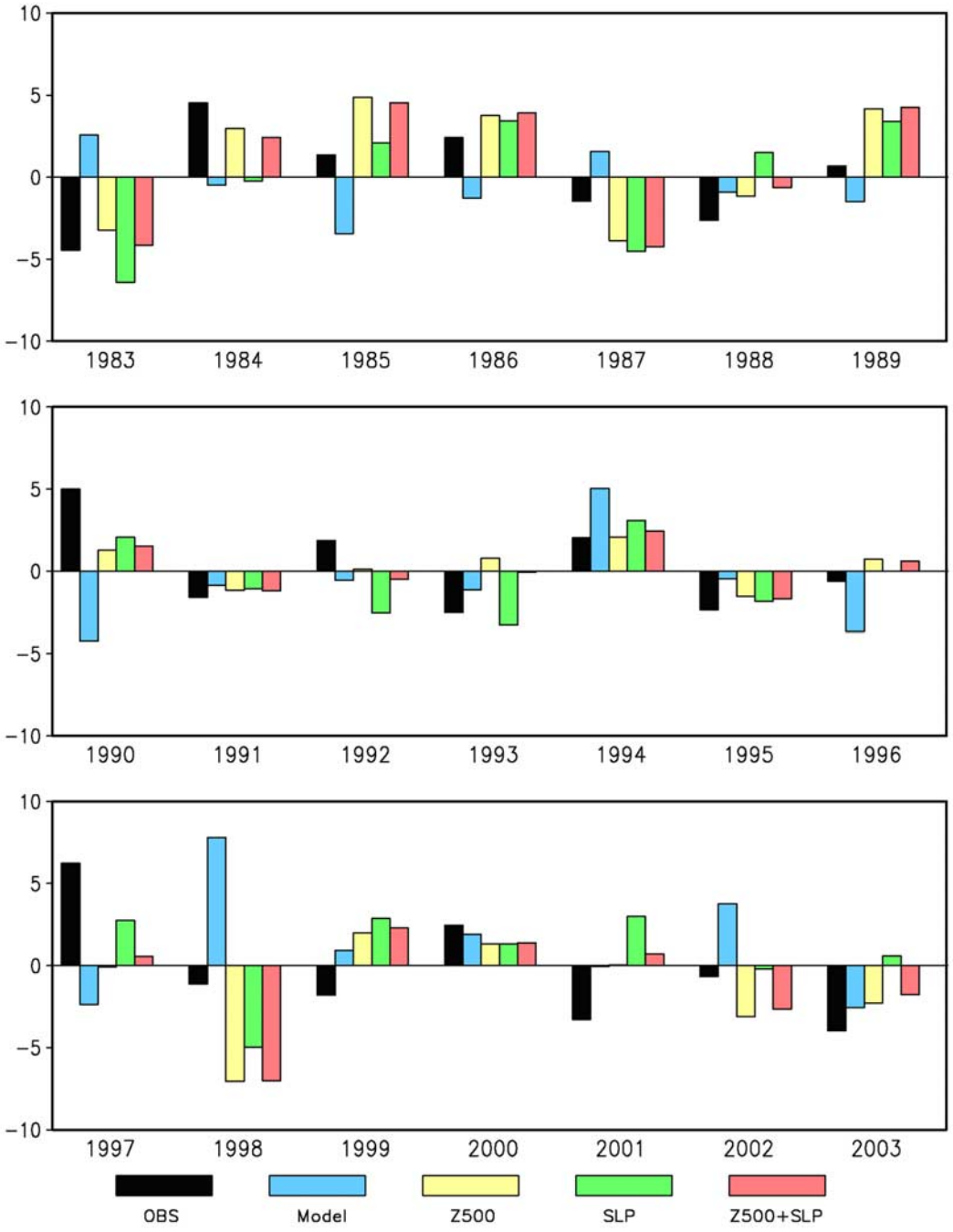

Figure 11. JJA precipitation, averaged over all stations (black), and the corresponding prediction based on different prediction schemes, for the period of 1983–2003 (blue: MME model output, yellow: downscaling prediction based on Z500, green: downscaling based on SLP, red: average of downscaling using Z500 and SLP.). Downscaling results are obtained from averages of downscaled prediction based on individual models. (Unit: mm/d).

the rainfall in northern Taiwan is the main factor for downscaling.

4. Summary and Discussion

[26] In this study, statistical downscaling based on GCM outputs of large-scale circulation variables is used to predict station rainfall over northern Taiwan. In particular, Z500 and SLP from six different global models are used as predictors. Downscaling is shown to considerably outperform global models in predicting regional precipitation. In general, downscaling predictions using Z500 give higher scores than those based on SLP as a predictor. This may be due to the inability on the part of some GCMs to represent a realistic

coupled pattern between SLP and station precipitation. On the other hand, the Z500 pattern coupled to station rainfall seems to be better captured in models. Also, it is shown that the mean of downscaling results based Z500 and SLP gives a more stable and skillful prediction. Overall, statistical downscaling can be a powerful method in extracting useful information on local climate variation from GCM outputs.

[27] Our results also suggest that the skill of downscaling is closely related to the following factors. (1) The ability of GCMs in capturing the coupled pattern between predictor and predictand: For example, for the JMA hindcast data, SLP (which is relatively well captured) can be regarded to be a better predictor when compared with Z500. (2) The degree of coupling between a model predictor and the predictand in the temporal sense: For instance, downscaling using NCEP data gives a poor skill. This may be related to the low correlation between the model large-scale circulation pattern and station rainfall, even though the model coupled patterns are realistic.

[28] **Acknowledgments.** The authors thank the Central Weather Bureau for providing the station data of precipitation. The authors also appreciate those institutes participating in the APCC multimodel ensemble operational system for providing the hindcast experiment data. Also, we thank Saji Njarackalazhikam Hameed, Ashok Karumuri, Mong-Ming Lu, Shu-Ping Weng, and Jyh-Wen Hwu for giving valuable comments on this study. The assistance from Doo-Young Lee, Daisuke Nohara, and Bong-Geun Song for data analysis is also appreciated.

References

Baek, S.-K., J.-H. Ryu, and S.-B. Ryoo (2002), Analysis of the CO_2 doubling experiment using METRI AGCM. Part I: The characteristics of regional and seasonal climate responses, *J. Korean Meteor. Soc.*, *38*, 465–477.

Barnston, A. G., Y. He, and M. H. Glantz (1999), Predictive skill of statistical and dynamical climate models in SST forecasts during the 1997–98 El Niño episode and the 1998 La Niña onset, *Bull. Am. Meteorol. Soc.*, *80*, 217–243, doi:10.1175/1520-0477(1999)080<0217:PSOSAD>2.0.CO;2.

Benestad, R. E. (2004), Empirical-statistical downscaling in climate modeling, *Eos Trans. AGU*, *85*(42), 417–422, doi:10.1029/2004EO420002.

Díez, E., C. Primo, J. A. García-Moya, J. M. Gutiérrez, and B. Orfila (2005), Statistical and dynamical downscaling of precipitation over Spain from DEMETER seasonal forecasts, *Tellus, Ser. A*, *57*(3), 409–423, doi:10.1111/j.1600-0870.2005.00130.x.

Feddersen, H., and U. Andersen (2005), A method for statistical downscaling of seasonal ensemble predictions, *Tellus, Ser. A*, *57*, 398–408, doi:10.1111/j.1600-0870.2005.00102.x.

Feddersen, H., A. Navarra, and M. N. Ward (1999), Reduction of model systematic error by statistical correction for dynamical seasonal predictions, *J. Clim.*, *12*, 1974–1989, doi:10.1175/1520-0442(1999)012<1974:ROMSEB>2.0.CO;2.

Giorgi, F., et al. (2001), Regional climate simulation-evaluation and projections, in *Climate Change 2001: The Scientific Basis*, edited by J. T. Houghton, 944 pp., Cambridge Univ. Press, New York.

Grotch, S. L., and M. MacCracken (1991), The use of general circulation models to predict regional climate change, *J. Clim.*, *4*, 286–303, doi:10.1175/1520-0442(1991)004<0286:TUOGCM>2.0.CO;2.

Hsu, H.-H., and S.-M. Lin (2007), Asymmetry of the tripole rainfall pattern during the East Asian summer, *J. Clim.*, *20*, 4443–4458, doi:10.1175/JCLI4246.1.

Kanamitsu, M., K. Tada, T. Kudo, N. Sata, and S. Isa (1983), Description of the JMA operational spectral model, *J. Meteorol. Soc. Jpn.*, *61*, 812–827.

Kang, I.-S., et al. (2002), Intercomparison of the climatological variations of Asian summer monsoon precipitation simulated by 10 GCMs, *Clim. Dyn.*, *19*, 383–395, doi:10.1007/s00382-002-0245-9.

Kang, I.-S., J.-Y. Lee, and C.-K. Park (2004), Potential predictability of summer mean precipitation in a dynamical seasonal prediction system with systematic error correction, *J. Clim.*, *17*, 834–844, doi:10.1175/1520-0442(2004)017<0834:PPOSMP>2.0.CO;2.

Kang, H., K.-H. An, C.-K. Park, A. L. S. Solis, and K. S. (2007), Multimodel output statistical downscaling prediction of precipitation in the Philippines and Thailand, *Geophys. Res. Lett.*, *34*, L15710, doi:10.1029/2007GL030730.

Kim, M.-K., I.-S. Kang, C.-K. Park, and K.-M. Kim (2004), Superensemble prediction of regional precipitation over Korea, *Int. J. Climatol.*, *24*, 777–790, doi:10.1002/joc.1029.

Lau, N.-C. (1985), Modeling the seasonal dependence of the atmospheric response to observed El-Nino in 1962–76, *Mon. Weather Rev.*, *113*, 1970–1996, doi:10.1175/1520-0493(1985)113<1970:MTSDOT>2.0.CO;2.

Liou, C.-S., J.-H. Chen, C.-T. Terng, F.-J. Wang, C.-T. Fong, T. E. Rosmond, H.-C. Kuo, C.-H. Shiao, and M.-D. Cheng (1997), The second-generation global forecast system at the central weather bureau in Taiwan, *Weather Forecasting*, *3*, 653–663.

Michaelsen, J. (1987), Cross-validation in statistical climate forecast models, *J. Clim. Appl. Meteorol.*, *26*, 1589–1600.

Murphy, A. H. (1988), Skill scores based on the mean square error and their relationships to the correlation coefficient, *Mon. Weather Rev.*, *116*, 2417–2424, doi:10.1175/1520-0493(1988)116<2417:SSBOTM>2.0.CO;2.

Murphy, J. (1999), An evaluation of statistical and dynamical techniques for downscaling local climate, *J. Clim.*, *12*, 2248–2256, doi:10.1175/1520-0442(1999)012<2256:AEOSAD>2.0.CO;2.

Rowell, D. P. (1998), Assessing potential seasonal predictability with an ensemble of multidecadal GCM simulations, *J. Clim.*, *11*, 109–120, doi:10.1175/1520-0442(1998)011<0109:APSPWA>2.0.CO;2.

Saha, S., et al. (2006), The NCEP climate forecast system, *J. Clim.*, *19*, 3483–3517, doi:10.1175/JCLI3812.1.

Shneerov, B. E., V. P. Meleshko, A. P. Solokov, D. A. Sheynin, V. A. Lyubanskaya, P. V. Sporyshev, V. A. Matyugin, V. M. Katzov, V. A. Govorkove, and T. V. Pavlova (1999), Global MGO model for atmospheric general circulation and upper oceanic layer, *Trudy MGO*, *554*, 1–123 (in Russian).

Sperber, K. R., and T. N. Palmer (1996), Interannual tropical rainfall variability in general circulation model simulations associated with the Atmosphere Model Intercomparison Project, *J. Clim.*, *9*, 2727–2750, doi:10.1175/1520-0442(1996)009<2727:ITRVIG>2.0.CO;2.

Sperber, K. R., et al. (2001), Dynamical seasonal predictability of the Asian summer monsoon, *Mon. Weather Rev.*, *129*, 2226–2247, doi:10.1175/1520-0493(2001)129<2226:DSPOTA>2.0.CO;2.

Tolstykh, M. A. (2003), Variable resolution version of the SL-AV global NWP model, *Russ. J. Num. An. & Math. Mod*, *18*, 347–361.

Von Storch, H., and F. W. Zwiers (1999). *Statistical Analysis in Climate Research*, 484 pp., Cambridge Univ. Press, New York.

Von Storch, H., E. Zorita, and E. Cubasch (1993), Downscaling of global climate estimates to regional scales: An application to the Iberian rainfall in wintertime, *J. Clim.*, *6*, 1161–1171, doi:10.1175/1520-0442(1993)006<1161:DOGCCE>2.0.CO;2.

Wang, W.-C., H.-H. Hsu, W.-S. Kau, X.-Z. Liang, LinHo, C.-T. Chen, A. N. Samel, C.-H. Tsou, P.-H. Lin, and K.-C. Ko (1998), GCM simulations of the East Asia climate, in *Proc. Third East Asia-West Pacific Meteorol. Clim. Conf.*, edited by C.-P. Chang, pp. 473–482, World Sci., Hackensack, N. J., 562 pp.

Wang, B., Q. Ding, X. Fu, I.-S. Kang, K. Jin, J. Shukla, and F. Doblas-Reyes (2005), Fundamental challenge in simulation and prediction of summer monsoon rainfall, *Geophys. Res. Lett.*, *32*, L15711, doi:10.1029/2005GL022734.

Wetterhall, F., S. Halldin, and C.-Y. Xu (2005), Statistical precipitation downscaling in central Sweden with the Analogue Method, *J. Hydrol.*, *306*, 174–190, doi:10.1016/j.jhydrol.2004.09.008.

Wilby, R. L., T. M. L. Wigley, D. Conway, P. H. Jones, B. C. Hewitson, J. Main, and D. S. Wilks (1998), Statistical downscaling of general circulation model output: A comparison of methods, *Water Resour. Res.*, *34*, 2995–3008, doi:10.1029/98WR02577.

Wilby, R. L., L. E. Hay, and G. H. Leavesley (1999), A comparison of downscaled and raw GCM output: Implications for climate change scenarios in the San Juan River Basin, Colorado, *J. Hydrol.*, *225*, 67–91, doi:10.1016/S0022-1694(99)00136-5.

Xu, C.-Y. (1999), From GCMs to river flow: A review of downscaling methods and hydrologic modeling approaches, *Prog. Phys. Geogr.*, *23*, 229–249.

C.-T. Chen and J.-L. Chu, Department of Earth Sciences, National Taiwan Normal University, No.88, Sec. 4, Tingzhou Road, Wenshan District, Taipei 116, Taiwan. (jlchu@rain.geos.ntnu.edu.tw)

H. Kang, C.-K. Park, and C.-Y. Tam, Science Division, APEC Climate Center (APCC), National Pension Corporation, Busan Bldg., Yeonsa 2-dong, Yeonje-gu, Busan 611-705, South Korea.